Traitement du Signal
Vol. 39, No. 6, December, 2022, pp. 2141-2147
Journal homepage: http://iieta.org/journals/ts

An Effective Kalman Based Hybrid Beamforming for Millimeter Wave Massive MIMO System by Using 2D Overlapped Partially Connected Sub-Array Structure

Gayatri D. Londhe*, Vaibhav S. Hendre

Department of Electronics and Telecommunication, G H Raisoni College of Engineering and Management, Pune 412207, India

Corresponding Author Email: gayatri.londhe.phdetc@ghrcem.raisoni.net

https://doi.org/10.18280/ts.390627

Received: 11 September 2022
Accepted: 10 December 2022

Keywords:
5G technology, hybrid beamforming, Kalman filter, millimeter-wave, partial connected subarray

ABSTRACT

In 5G mobile communication networks, millimeter-wave (mmWave) technology plays a key role. To deal with the problem of path loss that happens in the mmWave band, competent beamforming employing a large antenna array is required. Fully digital beamforming approaches currently require separate radio frequency chains (RF chains) for each antenna, which adds to the computational complexity and hardware expense. In a multi-user environment, fully digital beamforming suffers from a larger antenna array layout, whereas analog beamforming solutions are prone to numerous performance concerns. Hybrid beamforming, on the other hand, offers a promising solution for multi-user mmWave communication. This work proposes a two-dimensional overlapping partially connected (2D-OPC) sub-array structure to reduce the antenna structure's hardware complexity and cost. The suggested technique comprises several sub-arrays that are overlapped in 2D space in the form of a Uniform Planar Array (UPA). The suggested scheme's performance is assessed using Kalman-based hybrid beamforming, which exhibits a considerable increase in spectral efficiency when compared to existing hybrid beamforming techniques. The suggested technique, which uses Kalman based hybrid beamforming and 2D-OPC provides 3.14% and 4.96% improvement over the MMSE hybrid beamforming and ZF pre-coding technique respectively.

1. INTRODUCTION

5G technology uses high frequency bands to increase the broadcasting data rate with the help of improved bandwidth resources. In comparison to the 4G technology, 5G can now accommodate 1000× data packets. To achieve the 5G requirements, the present frequency range must be switched to the millimeter-wave frequency band (mm-wave- 30 to 300Gz), which has a wider bandwidth [1, 2]. The antenna array in an mm-wave system is extremely tiny due to the short wavelength and narrow beamwidth. The longest range between the user and the base station (BS) is a few hundred meters. Because of the tremendous increase in users and the increasing demand for a large amount of data, MIMO has got a lot of attention. It acts as a portal for increasing spectral efficiency in wireless networks. Massive MIMO (M-MIMO) is a setup of multi-user MIMO (MU-MIMO) setup [3]. The base station has a huge number of broadcast antenna elements, while the device has a large number of reception antenna elements. In M-MIMO, a base station with 100 or 1000 transmitter antenna elements simultaneously transmits data to tens or hundreds of reception antenna elements. Multiple antenna elements can help to improve spectral efficiency and capacity [4, 5]. Again, this results in interference, which can be mitigated by using beamforming antennas rather than standard antennas. M-MIMO offers enhanced throughput, low-power, low-cost components, and spectral capacity efficiency [6].

Beamforming is a signal processing technique for transmitting and receiving directional signals. The transmitter antennas distribute the signal in all directions while beamforming helps to target the wireless signal towards a single directional receiver. Beamforming aids in the transmission of a high-quality signal to a receiver. It aids in the reduction of interference generated by other devices attempting to catch other signals [7]. Beamforming techniques are classified as narrowband or wideband depending on the signal's bandwidth. In mm-wave beamforming, wideband beamforming has increased speed and capacity [8, 9]. Antenna elements are arranged in an array in which the beam steering towards a specific direction is taken into account while the rest of the beams are ignored in beamforming. Beamforming is a signal processing technique that improves spectral efficiency, system security, energy efficiency, and application to mm wavebands [10].

In most cases, two hybrid beamformer schemes are used such as the Fully Connected Structure (FCS) [11-13] and the Partially Connected Structure (PCS) [14-17]. Since each RF chain is linked to all antennas, the Fully Connected Structure (FCS) can attain maximum array gain, but it is not feasible because of the requirement of an enormous number of phase shifters and power amplifiers. However, each RF chain in the Partially Connected Structure (PCS), on the other hand, is coupled to a sub-array of antenna elements. The PCS considerably decreases the number of phase shifters, lowering each RF chain's beamforming gain.

The overlapping structure of the antenna sub-array helps to minimize the phase shifters to attain better spectral efficiency in mmWave communication. The 2D-OPC structure improves the spectral efficiency of the system as compared to PCS. It also reduces the hardware complexity as compared to FCS due to overlapping structure. Most of the existing subarray structures are founded on 1-D Uniform Linear Arrays (ULAs) [18, 19] and aims for single user broadcasting circumstance [20]. This paper presents different shapes of sub-array arranged in overlapped partially connected structure which is connected to multiple or single RF chains. The proposed structure helps to minimize the number of phase shifters while improving spectral efficiency.

Our research has made the following contributions, which are listed below:

·To investigate different 2-D Overlapped Partially Connected (2D-OPC) sub-array structures to minimize the hardware complexity and cost.

·To explore the effect of 2D-OPC sub-array using Kalman based hybrid beamforming to improve the spectral efficiency.

The remaining paper is structured as: Section II provides findings from the previous work on hybrid beamforming and sub-array structure. Section III gives a detailed description of the 2D-OPC sub-array structure scheme. Section IV depicts the Kalman based hybrid beamforming scheme to enhance spectral efficiency. Section V focuses on the experimental results and discussions. Finally, section VI concludes the paper and provides the future direction for the improvement of the scheme.

2. RELATED WORK

Various approaches for hybrid beamforming have been adopted in the past to boost the spectrum bandwidth of the communication network. Alkhateeb et al. [21] developed a combined strategy to identify the optimal RF combiner and beamformer to achieve improved spectrum efficiency. Additionally, they used Zero Forcing pre-coding (ZF) to reduce network disturbance. Nguyen et al. [22] also presented a hybrid MMSE pre-coding strategy for increasing spectral efficiency and reducing interference in mm-wave multiuser MIMO networks. For massive MIMO, Hussein et al. [23] proposed a low-complexity hybrid minimal mean square error (MMSE) pre-coding technique. It has resulted in a reduction in processing complexity as well as improved spectral efficiency. Mao et al. [24] looked into the minimum sum-mean-square error (min-SMSE) to design a digital combiner/pre-coder with a low bit error rate (BER). They also employed an over-sampling codebook (OSC) to design the analog combiner/pre-coder to reduce error. Li et al. [25] investigated the Gram-Schmidt algorithm and the MSME approach for dealing with inter-user interference in digital and analog beamforming with a considerably smaller channel matrix. Different block diagonalization approaches for hybrid beamforming have been proposed to increase spectral efficiency, reduce the computational burden, and reduce the Bit Error Rate (BER) [26, 27]. Yoo et al. [28] presented a two-dimensional overlapped partially connected (2D-OPC) sub-array structure to minimize the complexity and cost of the antenna structure along with ZF pre-coding. However, they have investigated very few types of partially connected sub-array structure and basic type of beamforming scheme that shows less improvement in sum rate compared with fully connected structure.

From the extensive survey of various hybrid beamforming techniques, it is observed that traditional hybrid beamforming techniques provide poor results for multi-user scenario and in case of interference. The previous schemes were often subjected to higher structural complexity and cost due to the fully connected structure of antenna elements. Several hybrid beamforming techniques suffer from larger computational complexity.

3. KALMAN BASED HYBRID BEAMFORMING MODEL

The schematic of the proposed scheme is illustrated in Figure 1. The proposed system uses 2D-OPC sub-array structure where each sub-array is connected to single or multiple RF chains. The 2D-OPC scheme is presented at the base station (transmitter) side as transmitter antennas are generally more than receiver antennas.

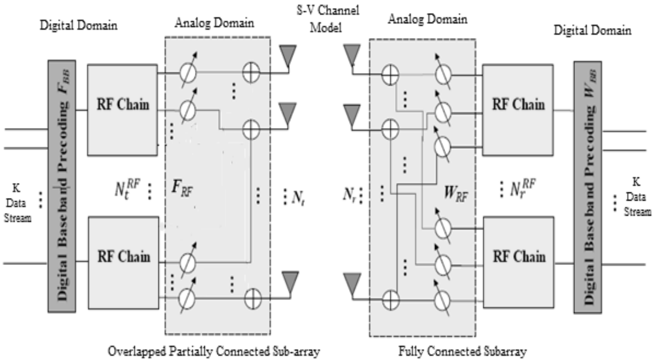

Figure 1. System model for proposed scheme

The proposed scheme uses different combinations of the sub-array structure for single or multiple users. The Saleh–Valenzuela (S-V) model [29] is used to characterize the equivalent channel that depicts the spatial characteristics of the mmWave communication system. The S-V model for *K* users can be formed using Eqns. (1) and (2).

$$H = [h_1, h_2, h_3, \dots., h_K]^T \tag{1}$$

where,

$$h_K^H = \sqrt{\frac{N_t N_r}{N_{cl} N_{ray}}} \sum_{i=1}^{Ncl} \sum_{j=1}^{Nray} G_{i,j} \,.\, a_r\left(\alpha_{i,j}^r, \beta_{i,j}^r\right) . \, a_t(\alpha_{i,j}^t, \beta_{i,j}^t) \tag{2}$$

where, N_t and N_r are the number of transmitter and receiver antennas, N_{cl} and N_{ray} symbolizes number of users and scatters respectively, *G* represents the path gain, a_r and a_t correspond to the antenna array vector at the transmitter (*t*) and receiver (*r*), *α* and *β* correspond to azimuth and elevation angle of arrival (AoA) and angle of departure (AoD) respectively. The azimuth angle (*α*) and elevation angle (*β*) are computed using Eq. (3). The proposed scheme considers the *V*×*H* UPA antenna sub-array with N_t antennas as the complete antenna structure.

$$\boldsymbol{a}(\alpha, \beta) = \frac{1}{\sqrt{N_t}} [1, \dots, e^{j\left(\frac{2\pi}{\lambda}\right) d(x sin\alpha sin\beta + y cos\beta)}, \dots, e^{j\left(\frac{2\pi}{\lambda}\right) d((H-1) sin\alpha sin\beta + (V-1) cos\beta)}]^T \tag{3}$$

where, x signifies the horizontal antenna index (x=1, 2, 3, ..., H-1) and y stands for vertical antenna index (y=1, 2, 3, ..., V-1). here, d and λ represent the distance between two adjacent antenna elements and transmission wavelength respectively.

The Kalman filter achieves better spectral efficiency by selecting the proper beamforming by reducing the error between broadcasted and estimated data [30]. Eq. (4) gives the state equation of the Kalman filter for the digital pre-coder matrix F_{BB}.

$$F_{BB}(z|z) = F_{BB}(z|z-1) + K(z)E\{diag[e(z)]\} \tag{4}$$

where, $K(z)$ characterizes the Kalman filter gain that is revised for every iteration using the covariance matrix of noise Q_z, the variance of Kalman state matrix $R(z)$, and the transpose of equivalent channel matrix H_e^H is given as:

$$K(z) = R(z|z-1)H_e^H[H_e R(z|z-1)H_e^H + Q_z]^{-1} \tag{5}$$

The variance of Kalman state matrix $R(z)$ is calculated as:

$$R(z|z) = [I - K(z)H_e]R(z|z-1) \tag{6}$$

The error $e(z)$ between transmitted $s(z)$ and estimated pre-coding matrix $\hat{s}(z)$ can be evaluated as:

$$e(z) = \frac{s(z) - \hat{s}(z)}{\|s(z) - \hat{s}(z)\|_F^2} \tag{7}$$

Kalman filter computes the error signal using effective channel matrix H_e and baseband pre-coder F_{BB} as:

$$E\{diag[e(z)]\} = \frac{I - \widehat{H_e}F_{BB}(z|z-1)}{\left\|I - \widehat{H_e}F_{BB}(z|z-1)\right\|_F^2} \tag{8}$$

The Kalman filter updates the hybrid pre-coder using Kalman filter gain, the equivalent channel matrix based on the Kalman filter can be updated as:

$$\begin{aligned} F_{BB}(z|z) &= F_{BB}(z|z-1) \\ &+K(z)\frac{I - \widehat{H_e}F_{BB}(z|z-1)}{\left\|I - \widehat{H_e}F_{BB}(z|z-1)\right\|_F^2} \end{aligned} \tag{9}$$

The performance of the proposed Kalman based hybrid beamforming using 2-D OPC sub-array structure for k^{th} user is estimated using the sum rate (R_k) in Eq. (10). Here, F_{RF} and F_{BB} correspond to the analog beamforming matrix and Kalman pre-coding matrix respectively, σ^2 represents identical noise variance for all users (K), and s_k describes the broadcasted symbol with K data streams which satisfies $[s.s^T]=I^K$.

$$R_k = log_2\left(1 + \frac{|h_k^T F_{RF} F_{BB} s_k|^2}{\sum_{i\neq k}^{K}|h_k^T F_{RF} F_{BB} s_i|^2 + \sigma^2}\right) \tag{10}$$

The overall sum rate (R) for all users is computed using Eq. (11).

$$R = \sum_{k=1}^{K} R_k \tag{11}$$

The analog beamforming matrix is given by:

$$F_{RF} = [f_1, f_{2,} \cdots . f_K] \tag{12}$$

where, $f_{k=}[f_{k,1}, f_{k,2}, \ldots, f_{k,N_t}]^T$ is the N_t×1 analog beamforming vector for the k-th UE with its elements defined as:

$$f_{k.m=}\begin{cases} \frac{1}{\sqrt{p}}\frac{[\boldsymbol{H}^H]_{k,m}}{|[\boldsymbol{H}^H]_{k,m}|}, & if\ m \in I_k \\ 0, & if\ m \notin I_k \end{cases} \tag{13}$$

for k=1, 2, …, K and m=1, 2, …, N_t.

The Kalman based hybrid pre-coding matrix is constructed using Eq. (14).

$$\begin{gathered} \min_{F_{RF},F_{BB}} E\left\|s(z) - \widehat{s(z)}\right\| \\ subjected\ to\ \left\|F_{rf}F_{BB}\right\|^2 = Ns \end{gathered} \tag{14}$$

4. 2D OVERLAPPED PARTIALLY CONNECTED SUB-ARRAY

In the fully connected structure (FCS), every antenna element is linked with all RF chains. Due to this FCS attains full beamforming gain for each RF chain. However, the FCS needs more phase shifters and power amplifiers which makes it less feasible for practical implementation. The FCS needs N_t×N_{rf} phase shifter where N_{rf} is the number of RF chains, which extensively adds more hardware complexity and cost. To minimize this drawback FCS system, partially connected systems (PCs) are often used where the whole antenna array is divided into dislodged sub-arrays and every sub-array is connected to a single RF chain. In PCS each RF chain is connected to a group of antennas called sub-arrays in a non-overlapping manner. The number of phase shifters required is equal to the number of antennas. The general topology of the partially connected structure is shown in Figure 2.

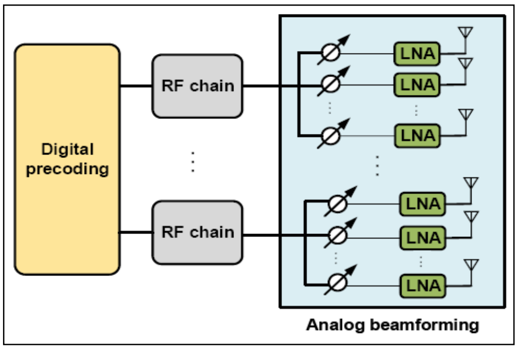

Figure 2. Partially connected structure

The PCS needs total N_t phase shifters as compared to FCS and thus minimizes the complexity of the system. The traditional PCS provides poor transmission performance because of the lower gain of RF chains.

To overcome the challenges faced by FCS and PCS, this article adopted the 2D-OPC sub-array structure given in the study of ref [28]. In the 2D-OPC sub-array, each sub-array is connected to the RF chain in such a way that the sub-array structure overlaps in both vertical and horizontal directions with the adjacent other sub-array. The internal principle of the 2D-OPC sub-array structure is the overlapping of antenna sub-arrays, which improves the spectral efficiency of the system as compared to PCS and reduces hardware complexity as compared to FCS. The number of phase shifters required for the 2D-OPC sub-array can be computed using Eq. (15):

$$N_{ps} = p \times N_{rf} \tag{15}$$

where, $p=v\times h$ represents the number of antenna elements in the sub-array.

In 2D-OPC the set of antenna elements of the sub-array linked with k^{th} RF chains are represented as:

$$I_k = \{i_1, i_2, \dots, i_p\} \tag{16}$$

In 2D-OPC, $c_{k,m}$ describes the particular antenna connection with the RF chain. If $c_{k,m}=1$, then the k^{th} RF chain and m antenna are linked with the phase shifter. Otherwise, if $c_{k,m}=0$, then the k^{th} RF chain and m antenna are not connected and a phase shifter is not required.

$$c_{k,m} = \begin{cases} 1, if m \in I_k \\ 0, if m \notin I_k \end{cases} \tag{17}$$

The 2D-OPC decides the position of overlapping sub-array. In 2D-OPC, various anchor points are selected using Eq. (18). The first anchor point for the sub-array is (1, 1) represent the first row position and first column position of the antenna element.

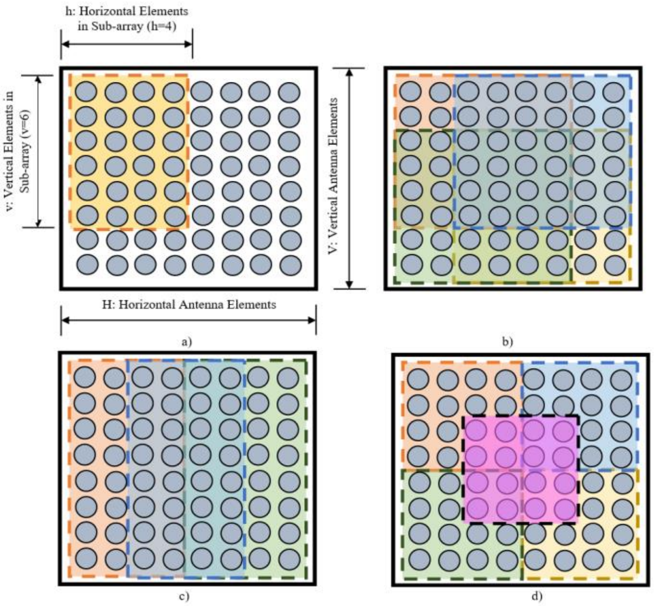

Figure 3. Design of 2D-OPC sub-array structure a) Structure of sub-array; b) Sub-array for v=6, h=6; c) Sub-array for v=8, h=4; d) Sub-array for v=4, h=4

Figure 3 illustrates the visualization various 2D-OPC sub-array structures such as (*v*=6, *h*=6), (*v*=8, *h*=4), and (*v*=4, *h*=4).

$$1 + \frac{(V-v)}{(Y-1)}(y-1), 1 + \frac{(H-h)}{(X-1)}(x-1) \tag{18}$$

here, *Y* and *X* represent the vertical and horizontal shift of the sub-array with *y*=1, 2, 3, …, *Y* and *x*=1, 2, 3, …, *X*. The sub-array in 2D-OPC is shifted uniformly over rows and columns of the base antenna array with the size of *V*×*H*.

The factors associated with values of $V$and H are spectral efficiency and data rate of the system. As referred in the literature the values of $V$and H are selected such that the distance between two antenna elements is considered as λ/2 where λ indicates wavelength. The size of the antenna array is 8×8 which is used here for analysis. Also, the number of elements in the transmitter antenna must be equal to the product of $V\times H$.

In Figure 3(b) the value of horizontal shift (*X*) and vertical shift (*Y*) is considered as 2 which leads to anchor point selection for 2D-OPC structure (*v*=6, *h*=6) over the array of *V*×*H* (V=8 and H=8) using Eq. (18) as (1,1), (1,3), (3,1), and (3,3). The first coordinate in the anchor point indicates the starting row position of the antenna element and the second coordinate indicates starting column position of the antenna element in the 2D-OPC sub-array.

5. RESULTS AND DISCUSSIONS

The proposed Kalman based hybrid beamforming using 2D-OPC sub-array structure model is implemented using a simulation model. The performance of the proposed hybrid beamforming is evaluated using the sum rate for various sub-array structures. The performance of the proposed hybrid beamforming is evaluated using the sum rate for various N_{rf}, N_{ps}, N_{ray}, *SNR,* and sub-array structures. The various parameters considered for the system simulation are described in Table 1.

Table 1. Parameter specifications of the proposed scheme

Parameter	Specification
Number of transmitter Antenna	64
Number of Receiver Antenna	16
Operating Frequency	28GHz
Number of RF chains	4-16
Number of phase shifters	64-324
Azimuth Angle	[0,2π]
Elevation Angle	[-π/2, π/2]
Number of users	5

Figure 4 shows the performance of the proposed scheme is evaluated for various antenna structures such as (*v*=6, *h*=6), (*v*=8, *h*=2), (*v*=8, *h*=4), and (*v*=4, *h*=4) for different RF chains for the multipath channel (Nrays=8). It is observed that the sub-array with (*v*=6, *h*=6) provides a better sum rate (86.27%) for 9 RF chains. Increasing the overlapping of sub-arrays in the antenna structure increases the number of available sub-array that show significant improvement in the sum rate despite of increase in RF chains. The sub-array structure with (v=4, h=4) provides multiple possibilities of the overlapping structures of the base antenna array but provides larger hardware complexity and lower sum rate compared with other sub-array with a higher number of antenna elements. The multipath channels (Nrays=8) provide better spatial diversity and result in an improved sum rate compared to the line of sight (LoS) channel model (Nray=1). Figure 5 shows the performance of proposed Kalman based hybrid beamforming based on different 2D OPC sub-array structure and distinct RF chains for LoS channel model (Nray=1). For the fully connected subarray, the Kalman based hybrid beamforming provides the sum rate of 94.12% and 84.66% for the multipath (Nray=8) and LoS (Nray=1) channel model.

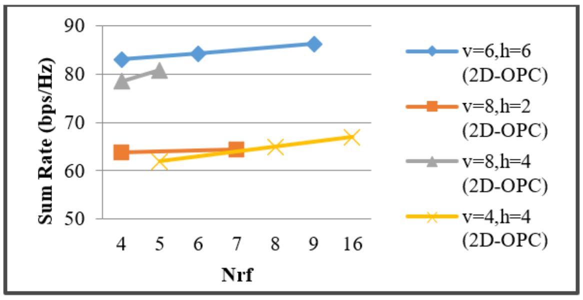

Figure 4. Performance of proposed scheme for Sum-rate versus the number of RF chains for different antenna structures for Kalman based hybrid beamforming using 2D-OPC (Nray=8)

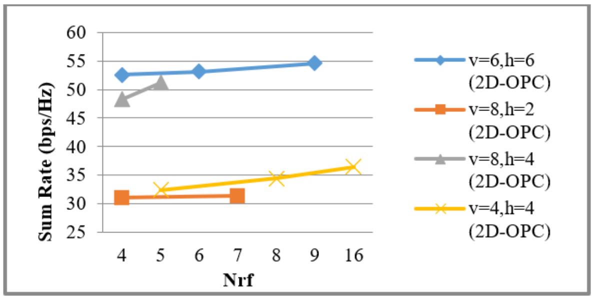

Figure 5. Performance of proposed scheme for Sum-rate versus the number of RF chains for different antenna structures for Kalman based hybrid beamforming using 2D-OPC (Nray=1)

Figures 6 and 7 provides the performance of the proposed Kalman based hybrid pre-coding for various sub-array structures (N_{rf}=4) for LoS and multipath channel model and different value of Signal to Noise (SNR). It shows improvement in the sum rate for increasing the value of SNR. The sub-array structure (v=6, h=6) depicts a higher sum rate compared to other sub-array structures with four RF chains.

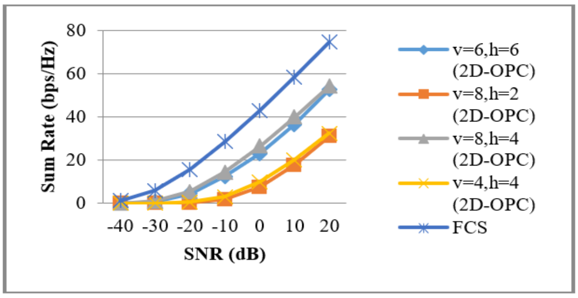

Figure 6. Sum rate vs SNR for various sub-array structures (Nray=1)

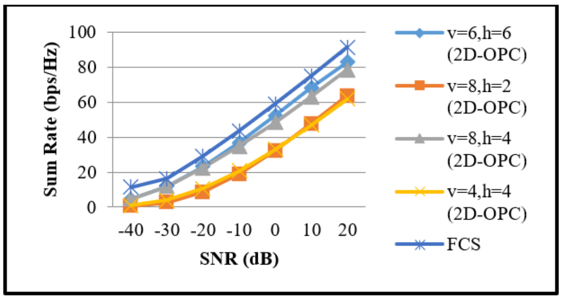

Figure 7. Sum rate vs SNR for various sub-array structures (Nray=8)

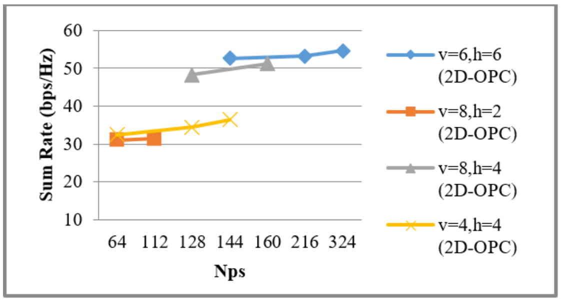

Figure 8. Sum rate vs number of phase shifters (Nps) for various sub-array structures (Nray=1)

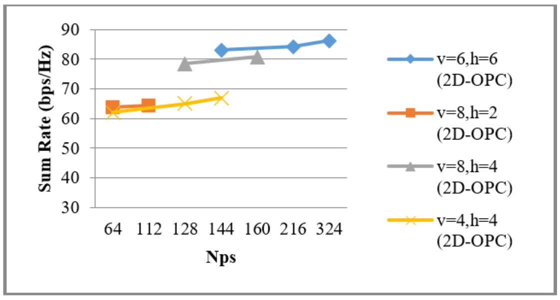

Figure 9. Sum rate vs number of phase shifters (Nps) for various sub-array structures (Nray=8)

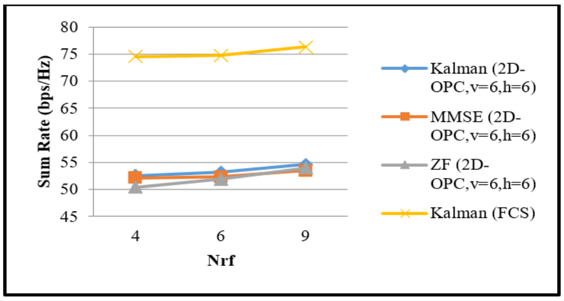

Figure 10. Performance comparison of proposed Kalman based hybrid beamforming based on 2D-OPC sub-array structure with MMSE and ZF hybrid beamforming (Nray=1)

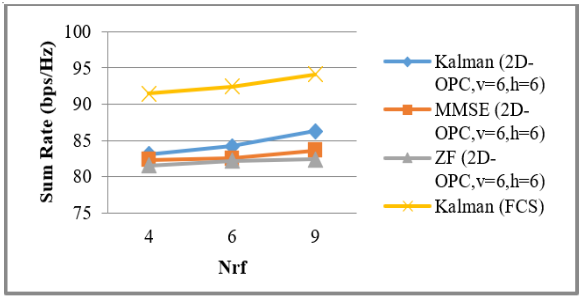

Figure 11. Performance comparison of proposed Kalman based hybrid beamforming based on 2D-OPC sub-array structure with MMSE and ZF hybrid beamforming (Nray=8)

A fully connected structure provides better performance compared with 2D-OPC as shown in Figure 6 and 7 but needs a large number of phase shifters which increases the hardware complexity and cost of the system. The 2D-OPC sub-array structure helps to minimize the number of phase shifters required for the hybrid beamforming which decreases the hardware cost and complexity. The performance of the proposed system for the different number of phase shifters of

Nray=1 and Nray=8 are given in Figure 8 and 9 respectively.

The effectiveness of the proposed Kalman based precoding based on 2D-OPC sub-array arrangement of base antenna sub-array is compared for the recent hybrid beamforming such as minimum mean square error (MMSE) hybrid beamforming and Zero-Forcing (ZF) hybrid beamforming techniques for mmWave communication system as given in Figures 10 and 11.

It is observed the robustness of Kalman filter under different SNR and channel model provides better error minimization capability between broadcasted and estimated signals. The proposed Kalman based hybrid beamforming achieves a sum rate of 86.27% for the 2D-OPC subarray (v=6, h=6) whereas for the fully connected structure it provides a sum rate of 94.12%.

The proposed 2D-OPC sub-array structure provides better results with the minimum number of RF chains and phase shifter that helps to minimize the hardware complexity compared with a fully connected hybrid beamforming scheme. The proposed Kalman based beamforming decreases the computational complexity due to the decline in the use of the number of RF chains and phase shifters of the beamforming technique and provides better performance for the multi-user system.

6. CONCLUSIONS

This paper presents Kalman based hybrid beamforming based on 2D overlapped partially connected sub-array base station antenna (2D-OPC) for mmWave communication system. The proposed scheme investigates various sub-array structures for the base station antenna to minimize the number of radio frequency chains that result in a reduction in the hardware complexity of the system. The proposed method tries to achieve the performance which is obtained using fully connected beamforming with a smaller number of RF chains. The proposed Kalman based hybrid beamforming scheme shows superior performance compared with the previous state of arts such as ZF pre-coding, MMSE hybrid beamforming, etc. It provides 3.14% and 4.96% improvement over the MMSE hybrid beamforming and ZF pre-coding technique respectively. The proposed system provides a good balance between the sum rate performance and hardware complexity of the system using a partially connected sub-array structure. Recently deep learning based algorithms are efficiently used for many signal processing applications and has given tremendous improvement in the results [31, 32]. In future the performance of hybrid beamforming can be enhanced using deep learning techniques.

REFERENCES

[1] Salih, A.A., Zeebaree, S.R., Abdulraheem, A.S., Zebari, R.R., Sadeeq, M.A., Ahmed, O.M. (2020). Evolution of mobile wireless communication to 5G revolution. Technology Reports of Kansai University, 62(5): 2139-2151.

[2] Liu, Y., Yagoub, M.C. (2020). Wideband millimeter wave planner sub-array with enhanced gain for 5G communication systems. In 2020 IEEE MTT-S International Conference on Numerical Electromagnetic and Multiphysics Modeling and Optimization (NEMO), Hangzhou, China, pp. 1-4. https://doi.org/10.1109/NEMO49486.2020.9343620

[3] Hendre, V., Murugan, M., Deshmukh, M., Ingle, S. (2017). Transmit antenna selection with optimum combining for aggregate interference in cognitive underlay radio network. Wireless Personal Communications, 92(3): 1071-1088. https://doi.org/10.1007/s11277-016-3593-1

[4] Hendre, V., Murugan, M., Chandgude, A.B. (2015). Multiple transmit antenna selection in MIMO-OSTBC system in Nakagami-m fading channel. Procedia Computer Science, 54: 558-565. https://doi.org/10.1016/j.procs.2015.06.064

[5] Londhe, G.D., Hendre, V.S. (2022). Review on beamforming techniques for millimeter wave massive MIMO. In Proceedings of the International e-Conference on Intelligent Systems and Signal Processing, pp. 291-303. https://doi.org/10.1007/978-981-16-2123-9_22

[6] Eldowek, B.M., Bauomy, N.A.E.S., El-Rabaie, E.S.M., Abd El-Atty, S.M., Abd El-Samie, F.E. (2021). A survey of 5G millimeter wave, massive multiple-input multiple-output, and vehicle-to-vehicle channel measurements and models. International Journal of Communication Systems, 34(16): e4830. https://doi.org/10.1002/dac.4830

[7] Yadav, R., Tripathi, A. (2020). A survey on hybrid, 3D, interference mitigation and secure data beamforming techniques for 5G system. Wireless Personal Communications, 114(1): 883-900. https://doi.org/10.1007/s11277-020-07397-w

[8] Sharma, A., Jha, R.K. (2021). A comprehensive survey on security issues in 5G wireless communication network using beamforming approach. Wireless Personal Communications, 119: 3447-3501. https://doi.org/10.1007/s11277-021-08416-0

[9] Gures, E., Shayea, I., Alhammadi, A., Ergen, M., Mohamad, H. (2020). A comprehensive survey on mobility management in 5G heterogeneous networks: Architectures, challenges and solutions. IEEE Access, 8: 195883-195913. https://doi.org/10.1109/ACCESS.2020.3030762

[10] Jijo, B.T., Zeebaree, S.R., Zebari, R.R., Sadeeq, M.A., Sallow, A.B., Mohsin, S., Ageed, Z.S. (2021). A comprehensive survey of 5G mm-wave technology design challenges. Asian Journal of Research in Computer Science, 8(1): AJRCOS.68058. https://doi.org/10.9734/ajrcos/2021/v8i130190

[11] Zhao, P., Wang, Z. (2018). Hybrid precoding for millimeter wave communications with fully connected subarrays. IEEE Communications Letters, 22(10): 2160-2163. https://doi.org/10.1109/LCOMM.2018.2859968

[12] El Ayach, O., Heath, R.W., Rajagopal, S., Pi, Z. (2013). Multimode precoding in millimeter wave MIMO transmitters with multiple antenna sub-arrays. In 2013 IEEE Global Communications Conference (GLOBECOM), pp. 3476-3480. https://doi.org/10.1109/GLOCOM.2013.6831611

[13] Dai, L., Gao, X., Quan, J., Han, S., Chih-Lin, I. (2015). Near-optimal hybrid analog and digital precoding for downlink mmWave massive MIMO systems. In 2015 IEEE International Conference on Communications (ICC), Atlanta, GA, USA, pp. 1334-1339. https://doi.org/10.1109/ICC.2015.7248508

[14] Majidzadeh, M., Moilanen, A., Tervo, N., Pennanen, H.,

Tölli, A., Latva-aho, M. (2017). Hybrid beamforming for single-user MIMO with partially connected RF architecture. In 2017 European Conference on Networks and Communications (EuCNC), Oulu, Finland, pp. 1-6. https://doi.org/10.1109/EuCNC.2017.7980696

[15] Hu, C., Liu, Y., Liao, L., Zhang, R. (2019). Hybrid beamforming for multi-user MIMO with partially-connected RF architecture. IET Communications, 13(10): 1356-1363. https://doi.org/10.1049/iet-com.2018.5830

[16] Wang, Y., Zou, W. (2020). Hybrid precoding design for millimetre wave systems with the partially-connected structure. IET Communications, 14(4): 561-567. https://doi.org/10.1049/iet-com.2019.0188

[17] Zhu, M., Xie, G., Qi, X. (2020). Low-complexity partially-connected hybrid precoding for massive MIMO systems. In 2020 IEEE Wireless Communications and Networking Conference (WCNC), Seoul, Korea (South), pp. 1-6. https://doi.org/10.1109/WCNC45663.2020.9120502

[18] Song, N., Yang, T., Sun, H. (2017). Overlapped subarray based hybrid beamforming for millimeter wave multiuser massive MIMO. IEEE Signal Processing Letters, 24(5): 550-554. https://doi.org/10.1109/LSP.2017.2681689

[19] Wang, Z., Zhu, J., Wang, J., Yue, G. (2018). An overlapped subarray structure in hybrid millimeter-wave multi-user MIMO system. In 2018 IEEE Global Communications Conference (GLOBECOM), Abu Dhabi, United Arab Emirates, pp. 1-6. https://doi.org/10.1109/GLOCOM.2018.8647446

[20] Hu, C.C., Zhang, J.H. (2018). Hybrid precoding design for adaptive subconnected structures in millimeter-wave MIMO systems. IEEE Systems Journal, 13(1): 137-146. https://doi.org/10.1109/JSYST.2018.2816927

[21] Alkhateeb, A., Leus, G., Heath, R.W. (2015). Limited feedback hybrid precoding for multi-user millimeter wave systems. IEEE Transactions on Wireless Communications, 14(11): 6481-6494. https://doi.org/10.1109/TWC.2015.2455980

[22] Nguyen, D.H., Le, L.B., Le-Ngoc, T. (2016). Hybrid MMSE precoding for mmWave multiuser MIMO systems. In 2016 IEEE international conference on communications (ICC), Kuala Lumpur, Malaysia, pp. 1-6. https://doi.org/10.1109/ICC.2016.7510844

[23] Hussein, M.K., Khamiss, N.N. (2020). Multi-user massive MIMO systems based on hybrid analog-digital beamforming for millimeter-wave communications. Int. Journal of Intelligent Engineering and Systems, 13(5): 408-415.

[24] Mao, J., Gao, Z., Wu, Y., Alouini, M.S. (2018). Over-sampling codebook-based hybrid minimum sum-mean-square-error precoding for millimeter-wave 3D-MIMO. IEEE Wireless Communications Letters, 7(6): 938-941. https://doi.org/10.1109/LWC.2018.2839723

[25] Li, J., Xiao, L., Xu, X., Zhou, S. (2016). Robust and low complexity hybrid beamforming for uplink multiuser mmWave MIMO systems. IEEE Communications Letters, 20(6): 1140-1143. https://doi.org/10.1109/LCOMM.2016.2542161

[26] Ni, W., Dong, X. (2015). Hybrid block diagonalization for massive multiuser MIMO systems. IEEE Transactions on Communications, 64(1): 201-211. https://doi.org/10.1109/TCOMM.2015.2502954

[27] Hu, C., Liu, J., Liao, X., Liu, Y., Wang, J. (2017). A novel equivalent baseband channel of hybrid beamforming in massive multiuser MIMO systems. IEEE Communications Letters, 22(4): 764-767. https://doi.org/10.1109/LCOMM.2017.2787715

[28] Yoo, J., Sung, W., Kim, I.K. (2021). 2D-OPC subarray structure for efficient hybrid beamforming over sparse mmwave channels. International Journal of Antennas and Propagation, 2021: 6680566. https://doi.org/10.1155/2021/6680566

[29] Mohammed, S.L., Alsharif, M.H., Gharghan, S.K., Khan, I., Albreem, M. (2019). Robust hybrid beamforming scheme for millimeter-wave massive-MIMO 5G wireless networks. Symmetry, 11(11): 1424. https://doi.org/10.3390/sym11111424

[30] Vizziello, A., Savazzi, P., Chowdhury, K.R. (2018). A Kalman based hybrid precoding for multi-user millimeter wave MIMO systems. IEEE Access, 6: 55712-55722. https://doi.org/10.1109/ACCESS.2018.2872738

[31] Rehman, A., Butt, M.A., Zaman, M. (2022). Liver lesion segmentation using deep learning models. Acadlore Trans. Mach. Learn., 1(1): 61-67. https://doi.org/10.56578/ataiml010108

[32] Wawage, P., Deshpande, Y. (2022). Real-Time prediction of car driver's emotions using facial expression with a convolutional neural network-based intelligent system. Acadlore Trans. Mach. Learn., 1(1): 22-29. https://doi.org/10.56578/ataiml010104